Atmos. Chem. Phys., 26, 16571–16582, 2026
https://doi.org/10.5194/acp-26-16571-2026
© Author(s) 2026. This work is distributed under
the Creative Commons Attribution 4.0 License.

Atmospheric Chemistry and Physics
Open Access
EGU

An overlooked kinetic relaxation in the formation of sesquiterpene-derived criegee intermediates

Hengjia Ou[1,★], Yao Li[2,★], Yuqing Sha[3], Hui Zhou[4,5], Jingkun Jiang[6], and Kunpeng Chen[4,6]

[1]Guangzhou Institute of Tropical and Marine Meteorology, China Meteorological Administration, Guangzhou 510640, China
[2]Yantai Meteorological Bureau, Yantai, Shandong 264003, China
[3]Fuyang Meteorological Bureau, Fuyang, Anhui 236000, China
[4]Key Laboratory for Thermal Science and Power Engineering of Ministry of Education, Beijing Key Laboratory of CO_2 Utilization and Reduction Technology, Department of Energy and Power Engineering, Tsinghua University, Beijing 100084, China
[5]Shanxi Research Institute for Clean Energy, Tsinghua University, Shanxi, Taiyuan 030000, China
[6]State Key Laboratory of Regional Environment and Sustainability, School of Environment, Tsinghua University, Beijing 100084, China
★These authors contributed equally to this work.

Correspondence: Kunpeng Chen (chenkp@tsinghua.edu.cn)

Received: 5 June 2026 – Discussion started: 6 July 2026
Revised: 23 October 2026 – Accepted: 9 November 2026 – Published: 20 November 2026

Abstract. Sesquiterpene ozonolysis contributes to secondary organic aerosol (SOA) formation by producing Criegee intermediates (CIs) via primary ozonide (POZ) decomposition. POZs are generally non-thermalized and thus assumed not to influence the formation rate constants of CIs, yet a fraction of sesquiterpene-derived POZs could be thermalized under atmospheric conditions, which is typically overlooked but potentially affects CI formation kinetics. This study derived a POZ-explicit kinetic model for sesquiterpene-derived CI formation, showing that the CI formation rate constant is initially unstable but gradually approaches a plateau equal to the rate constant of sesquiterpene ozonolysis. Such behavior is called "kinetic relaxation" and the relaxation timescale, as shown by our model, can be extended by cold surges but diminished by heatwaves. Our results revealed that kinetic relaxation occurs mainly in the thermalized POZs; the fractions of thermalized POZs were estimated to be less than 2 % for α-cedrene, up to $\sim$ 34 % for α-copaene, and over 90 % for β-caryophyllene. The high thermalized fractions of β-caryophyllene POZs lead to CI formation rate constants at room temperature that are 3–5 orders of magnitude lower than those calculated without kinetic relaxation. Our findings suggest that kinetic relaxation may enable reactions between thermalized POZs and atmospheric radicals, providing a new perspective on the fate of sesquiterpenes in atmospheric ozonolysis.

1 Introduction

Atmospheric Criegee intermediates (CIs) are produced from the ozonolysis of airborne alkenes such as terpenes (Criegee, 1975; Johnson and Marston, 2008), but whether the formation rate of CIs equals the rate of ozonolysis is still a question. The formation of CIs from reactions between terpenes and ozone (O_3) contributes to the atmospheric oxidation capacity (Khan et al., 2018; Chhantyal-Pun et al., 2020), which governs the formation of O_3-initiated secondary organic aerosols (SOAs) (Zhao et al., 2015; Zhao et al., 2016; Gong and Chen, 2021). CI chemistry produces hydroxyl (OH) radicals and organic hydroperoxides (ROOHs) (Docherty et al., 2005; Reinnig et al., 2009; Donahue et al., 2011; Iyer et al., 2021), which further boost the formation of oxygenated species (e.g., carbonyls, alcohols) with high

molecular weights in SOAs (Dekermenjian et al., 1999; Jaoui et al., 2003, 2004, 2013, 2017; Kanawati et al., 2008; Reinnig et al., 2009). The formation rate of CIs is determined not only by the concentrations of O_3 and terpenes but also by the formation rate constant (k_{CI}).

The value of k_{CI} is generally assumed equal to the ozonolysis rate constant (k_{oz}) in the literature (Taatjes et al., 2014; Cox et al., 2020). In principle, terpene ozonolysis first forms stabilized prereactive complexes (SPCs) and subsequently generates primary ozonides (POZs), which further decompose into CIs (Donahue et al., 2011; Vereecken and Francisco, 2012; Taatjes et al., 2014). The quantity k_{CI} refers to the projection from the reactants (sesquiterpenes and O_3 in this study) to CIs (Scheme I), and k_{oz} refers to the projection from the reactants to POZs (Ou and Chen, 2025; Ou et al., 2026). Given the high exothermic energy ($\sim$ 50–60 kcal mol^{-1}) from O_3 addition to the C=C double bond (Nangia and Benson, 1980; Cremer, 1981; Chuong et al., 2004; Johnson and Marston, 2008), POZs are typically in their vibrationally excited states to rapidly produce CIs under normal atmospheric conditions (Chuong et al., 2004; Hakala and Donahue, 2023). In this case, the conversion from POZs to CIs is expected to be far from thermal equilibrium so that the reaction proceeds more like SPCs overcoming the energy barrier corresponding to k_2 and directly produce CIs (Scheme II).

$$\text{Sesquiterpene} + O_3 \xrightarrow{k_{CI}} \text{CIs} \quad \text{(I)}$$

$$\text{Sesquiterpene} + O_3 \underset{k_{-1}}{\overset{k_1}{\rightleftharpoons}} \text{SPCs} \xrightarrow{k_2} \text{POZs (excited)} \xrightarrow{\text{rapid}} \text{CIs} \quad \text{(II)}$$

$$\text{Sesquiterpene} + O_3 \underset{k_{-1}}{\overset{k_1}{\rightleftharpoons}} \text{SPCs} \xrightarrow{k_2} \text{POZs (thermalized)} \xrightarrow{k_3} \text{CIs} \quad \text{(III)}$$

However, if POZs are fully thermalized, k_{CI} and k_{oz} are not necessarily interchangeable (Scheme III). This will not happen for all of the small alkenes and even C_{10} molecules (e.g., monoterpenes) in the air, but for C_{15} molecules such as sesquiterpenes, a fraction of them can be thermalized under atmospheric conditions (Chuong et al., 2004). In this case, there is no guarantee that k_{CI} can be equal to k_{oz}. The influence of k_3 on k_{CI} is largely overlooked from the thermalized POZs. To address this concern, the community may require a rigorous approach to resolving the rate constant of CI formation by explicitly considering the POZ-to-CI conversion.

This study discloses a previously unrecognized phenomenon, termed "kinetic relaxation", by explicitly elucidating the relationship between k_{CI} and k_{oz}. Kinetic relaxation refers to a transient deviation of k_{CI} from k_{oz}. We selected CIs from sesquiterpene ozonolysis as our case study for three reasons: (1) the rate constants of sesquiterpene ozonolysis mostly show no dependence on air pressure in the troposphere; (2) the large molecular size of sesquiterpenes may keep the SPCs collisionally stabilized (Wong et al., 2003; Yao et al., 2017; Ou and Chen, 2025); (3) sesquiterpenes are C_{15} molecules such that their ozonolysis yields a fraction of thermalized POZs under atmospherically relevant conditions (Chuong et al., 2004). The sesquiterpene-derived CIs thus serve as a simplified system that maintains a clear "double-well" potential energy surface along the CI formation mechanism (Donahue et al., 2011; Vereecken and Francisco, 2012; Taatjes et al., 2014), which is key to understanding the kinetic relaxation. The studied sesquiterpenes involve α-cedrene, α-copaene, β-caryophyllene, α-farnesene and β-farnesene, which are representative in the troposphere and emitted from vegetation in forests and farms (Lwande et al., 1989; Arey et al., 1995; Duhl et al., 2008; Yee et al., 2018; Frazier et al., 2022; Chen et al., 2024). Ozonolysis represents the predominant fate of these compounds (Shu and Atkinson, 1995; Richters et al., 2015; Frazier et al., 2022), and most of their CIs (e.g., $\sim$ 88 % for α-cedrene and $>$ 60 % for β-caryophyllene) can be stabilized in the atmosphere (Winterhalter et al., 2009; Nguyen et al., 2009; Yao et al., 2014). We estimated all the kinetic parameters with a computational approach that can replicate the temperature-dependent ozonolysis rate constants of α-cedrene (Fig. S1 in the Supplement) and β-caryophyllene (Ou and Chen, 2025). The influence of temperature variations on sesquiterpene ozonolysis kinetics as well as the relaxation timescale is also explored. The atmospheric implications of kinetic relaxation in the sesquiterpene-derived CI formation kinetics are further discussed.

2 Methods

2.1 Kinetics of Sesquiterpene Ozonolysis

The rate constant of sesquiterpene ozonolysis (k_{oz}) can be expressed by Eq. (1), as presented in our previous studies (Ou and Chen, 2025; Ou et al., 2026).

$$k_{oz} = k_1 \cdot \sum_i \left[p_i \cdot \left(\frac{k_{2,i}}{k_{-1,i} + k_{2,i}} \right) \right] \quad (1)$$

here k_1 is the bimolecular collision rate constant of the sesquiterpene molecule and O_3, which is calculated by the collision theory; p_i is the branching ratio of the ith SPC arisen from the bimolecular collisions, which is also corresponding to the ith POZ; $k_{-1,i}$ and $k_{2,i}$ are the rate constants of the backward dissociation of the ith SPC and the forward formation of the ith POZ, respectively. All these quantities can be affected by temperature variations, and the ratio $k_{2,i}/(k_{-1,i} + k_{2,i})$ serves as the main factor to control the temperature dependence of the ith POZ formation kinetics (Ou and Chen, 2025). Since the temperature-dependent ozonolysis rate constants of β-caryophyllene, α-farnesene and β-farnesene have been quantified by previous experimental measurements (Kim et al., 2011; Gao et al., 2022),

Eq. (1) was employed to estimate the temperature-dependent ozonolysis rate constants of α-cedrene and α-copaene.

2.2 Kinetics of CI Formation

The computation of k_{CI} is based on the steady-state concentration of SPCs (Sect. S1 in the Supplement), which is supported by experimental measurements (Talukdar et al., 2003; Davis et al., 2005; Ou and Chen, 2025). The expression of k_{CI} is approximated by Eq. (2), wherein $f_{CI,i}$ is the projection factor for the ith CI, as given by Eq. (3), if the initial concentrations of all POZs are zero.

$$k_{CI} \approx k_{oz} \cdot \sum_i f_{CI,i} \tag{2}$$

$$f_{CI,i} = r_i \cdot (1 - e^{-k_{3,i} \cdot t}) \tag{3}$$

In Eq. (3), t is time after ozonolysis starts, r_i is the steady-state branching ratio of the ith CI formation, which satisfies $\sum_i r_i = 1$ (Sect. S1), and $k_{3,i}$ is the rate constant of the ith CI formation from POZ decomposition. When the initial concentrations of POZs are not zero, $f_{CI,i}$ should be implemented with a scale factor s_i (Sect. S2). Equation (3) also shows that, when t equals 0, $f_{CI,i}$ also equals 0 (Sect. S1); if the ith POZ pre-exists before the ozonolysis (i.e., s_i shows up in $f_{CI,i}$), the value of $f_{CI,i}$ will equal $r_i \cdot s_i$ when t equals 0 (Sect. S2). Regardless of the s_i, if t is infinitely large, $f_{CI,i}$ will equal 0 so that k_{CI} will converge with k_{oz} (Sects. S1 and S2). Equations (2) and (3) show that k_{CI} is not equal to k_{oz} at the beginning of ozonolysis, but k_{CI} approaches k_{oz} after a period of relaxation. The projection factors $f_{CI,i}$ represent the kinetic relaxation of each CI generated from sesquiterpene ozonolysis.

2.3 Thermodynamic and Kinetic Computation

The thermodynamic parameters such as zero-point energy (ZPE) and vibrational frequencies were computed by the ORCA 5.0.4 software (Neese, 2012). Vibrational analysis based on the optimized structures was conducted by the density functional theory (DFT) with the M06-2X functional (Zhao and Truhlar, 2008) and the def2-TZVP basis set (Weigend and Ahlrichs, 2005). The RIJCOSX approximation was also employed to accelerate all the calculations (Neese et al., 2009). Single-point energy was computed by using the DLPNO-CCSD(T) method with the def2-TZVPP basis set (Riplinger and Neese, 2013; Weigend and Ahlrichs, 2005), accelerated by the RIJCOSX algorithm as well. For benchmarking, the same DLPNO-CCSD(T) method was also applied with the cc-pVTZ basis set (Dunning, 1989; Weigend et al., 2002), and the resulting energy barriers were 0.3–0.5 kcal mol^{-1} higher than those obtained by using def2-TZVPP (Table S1 in the Supplement). The thermodynamic parameters were used to calculate p_i, $k_{-1,i}$, $k_{2,i}$, and $k_{3,i,j}$ within the temperature range of 243–323 K and the temperature increment of 5 K using the J-resolved microcanonical variational transition state theory (mVTST) incorporated in the Multiwell 2023 program (Barker, 2009, 2001). Detailed computation procedures and accuracy tests were described in our previous study (Ou and Chen, 2025).

The decomposition kinetics of POZs was estimated using the RRKM/ME computation (i.e., Rice–Ramsperger–Kassel–Marcus theory/master equation) by the Multiwell 2023 program (Barker, 2009, 2001). The pressure was set as 1.0 atm, and the surrounding collider was nitrogen gas (N_2) with the Lennard–Jones (LJ) parameters (σ and ϵ/k_B) of 3.70 Å and 85 K (Weaver and Alexeenko, 2015). Since the LJ parameters for the studied POZs are unavailable, our calculations assumed 6.77 Å and 365 K for α-cedrene, α-copaene, β-caryophyllene (hydrocarbons with several alkyl branches) and 8.02 Å and 362 K for α-farnesene and β-farnesene (long-chain hydrocarbons) (Hippler et al., 1983). The exponential model was employed for deactivation collision (Tardy and Rabinovitch, 1977; Barker et al., 2001), with the energy loss of deactivation collision set to 500 cm^{-1} (Chuong et al., 2004). The density of states was computed by the DenSum code incorporated in the program. Details of the RRKM/ME setup in the Multiwell 2023 program are available in Sect. S1.

2.4 Arrhenius Fitting of Temperature Dependence

The computed $k_{-1,i}$, $k_{2,i}$, and $k_{3,i,j}$ were further fitted by the Arrhenius equation $k(T) = A \cdot \exp(-E_a/(RT))$, wherein A is the pre-exponential factor, E_a is the activation energy, and R is the ideal gas constant. The temperature dependence of $k_{-1,i}$, $k_{2,i}$, and $k_{3,i,j}$ is controlled by the value of E_a. The computed k_{oz} was fitted by the modified Arrhenius equation (Eq. 4).

$$k_{oz} \approx F_{oz} \cdot \left(\frac{T}{298}\right)^m \cdot e^{\Theta/T} \tag{4}$$

here F_{oz} is the temperature-independent constant for ozonolysis, m is the constant for temperature dependence of the power-law factor, and Θ is the constant for temperature dependence of the exponential factor.

3 Results and Discussions

3.1 The Origin of Kinetic Relaxation

The kinetic relaxation was found when we explicitly derived the kinetic model of CI formation. As suggested in the literature (Taatjes et al., 2014; Cox et al., 2020), the rate constant for CI formation was previously assumed to be equal to that of ozonolysis. Such an assumption treats the process from sesquiterpene ozonolysis to CI formation as a balance of inflow and outflow, but since this process is a consecutive reaction intermediated by SPCs and POZs, the rate of sesquiterpene consumption and the rate of CI formation are

in principle not always the same. Stepwise kinetics related to SPCs and POZs should be explicitly handled.

Here SPCs are assumed to be at steady-state concentrations (Fig. 1A and Sect. S2), which supports the time-dependent concentrations of POZs (Sect. S3). The concentration of each POZ is initially zero, subsequently increases along with ozonolysis time, and asymptotically approaches a plateau value that represents the steady-state POZ concentration (Fig. 1B). The time-dependent concentration of POZs causes k_{CI} to also vary with time (Sect. S3). The well-established mechanism of CI formation indicates that CIs are not directly generated from the reactive collision between alkenes and O_3 but from the decomposition of POZs (Criegee, 1975; Donahue et al., 2011; Taatjes et al., 2014; Vereecken and Francisco, 2012). So, in principle, k_{CI} should be a parameter of energy distribution of POZs. At the beginning of ozonolysis, k_{CI} is also zero unless pre-existing POZs are present before the ozonolysis (Sect. S4). The value of k_{CI} increases over time and asymptotically approaches its plateau value (Fig. 1C), which is exactly k_{oz} (Sect. S3). Our deductive results suggest that only when both SPCs and POZs are at their steady-state concentrations can k_{CI} be equal to k_{oz}.

3.2 Kinetics of Sesquiterpene Ozonolysis

The ozonolysis kinetics is mainly determined by the kinetic competition between SPC dissociation (k_{-1}) and POZ production (k_2). Taking α-cedrene and α-copaene as examples, both molecules have only one C=C double bond and both have two sites for ozonolysis (Fig. 2A). Since each POZ has two conformers, there are totally four POZs can be formed for α-cedrene or α-copaene (Fig. S2). The POZ production tendency is quantified by the ratio $k_2/(k_{-1}+k_2)$ (Figs. S3 and S4), wherein the predominant channels for POZ production as well as CI formation are shown here (Fig. 2B and C). The comparisons of activation energies ($E_a(k_{-1})$ and $E_a(k_2)$) from the Arrhenius fitting are also provided (Fig. 3, Table S2).

For α-cedrene, site 2 dominates the production of POZs. The values of $E_a(k_2)$ and $E_a(k_{-1})$ are comparable at site 2, with SPC2-1 uniquely showing $E_a(k_2) < E_a(k_{-1})$ (Fig. 3A). The resultant $k_2/(k_{-1}+k_2)$ shows different temperature dependence for SPC2-1 and SPC2-2 (Fig. S3C and D), with the case in SPC2-1 remaining largely stable across temperatures. Similarly, the production of POZs from α-copaene exclusively occurs at site 2 (Table S3). The ratio $k_2/(k_{-1}+k_2)$ at site 2 does not decrease significantly with declining temperature (Fig. S4C and D). Since branching ratios of all the POZs minorly vary with temperature (Table S3), the ozonolysis channels of α-cedrene and α-copaene are very stable across a wide temperature range.

The ozonolysis kinetics of α-cedrene and α-copaene exhibit only weak temperature dependence (Fig. S5A). Despite the wide temperature range, their k_{oz} remain within a narrow interval (~ 1.5–1.7×10^{-16} cm^3 molec.$^{-1}$ s^{-1}). The analytical fitting based on the modified Arrhenius equation gives $k_{oz} = 3.8 \times 10^{-16} \times (T/298)^{-0.7} \times \exp(-236.6/T)$ for α-cedrene and $k_{oz} = 2.5 \times 10^{-16} \times (T/298)^{-0.4} \times \exp(-139.6/T)$ for α-copaene (Fig. S6). In these expressions, the exponential terms increase with temperature, whereas the temperature-dependent pre-exponential factors decrease (Fig. S7). This phenomenon is different from those of β-caryophyllene and farnesenes, wherein β-caryophyllene exhibits an increasing exponential factor as temperature increases, while farnesenes show decreasing exponential factors (Fig. S7A) (Kim et al., 2011; Gao et al., 2022). Notably, their pre-exponential factors remain unchanged along with the temperature variations, in contrast to the compensating trends observed for α-cedrene and α-copaene (Fig. S7B). Among the studied sesquiterpenes, α-cedrene and α-copaene are very resistant to temperature variations regarding their k_{oz} values. The resistant k_{oz} indicates that the POZ production flux is correspondingly stable.

3.3 Kinetics of POZ Decomposition

The decomposition kinetics of POZs is studied by plotting the decay of POZ and the formation of resultant CIs is shown along with time (Fig. 4). The α-cedrene-derived and α-copaene-derived POZ concentrations start to decay at $\sim 10^{-12}$ s with the half-lives at $\sim 10^{-10}$–10^{-9} s (Fig. 4A–D). Temperature variations change little on the concentration profiles of both POZs and the resultant CIs. The decomposition kinetics of the predominant POZs derived from β-caryophyllene, using the computed structures obtained from our previous studies (Ou and Chen, 2025), shows different concentration profiles (Fig. 4E and F). Unlike the nearly complete decomposition of α-cedrene-derived POZs, the decay of β-caryophyllene-derived POZs is greatly hindered, with over 90 % of the initial POZs remaining undecomposed (Fig. 4E and F).

The influence of temperature variation on the concentration profiles of POZs and CIs may strongly depend on the structures of sesquiterpenes. Our results show negligible differences in the POZ and CI concentration profiles for α-cedrene (Fig. 4A and B) and β-caryophyllene (Fig. 4E and F), whereas a notable influence is observed for α-copaene (Fig. 4C and D). Specifically, lower temperatures (e.g., 243 K) suppress the decomposition of α-copaene-derived POZs, resulting in a higher fraction of thermalized POZs and a lower yield of CIs than at higher temperatures (e.g., 318 K). Even between the two POZs derived from α-copaene, the temperature sensitivity is not uniform, with the suppression of CI formation at lower temperature being more pronounced for POZ2-1. Our results suggest that the formation fluxes of different CIs from even the same precursor may vary differently as temperature changes.

Our results further reveal that, although each POZ can decompose via two channels to form two CI isomers (Fig. 5),

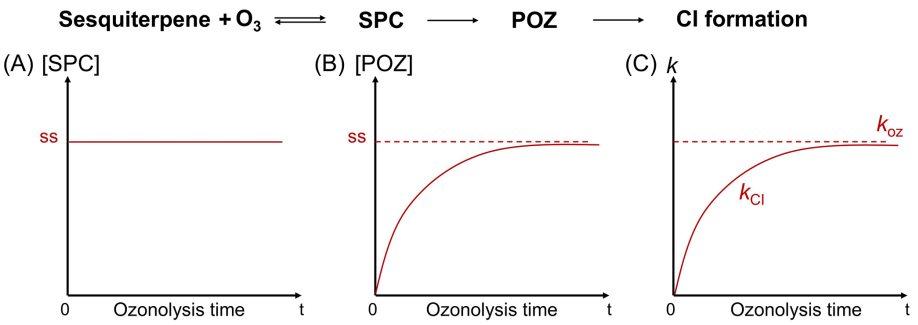


Figure 1. The origin of kinetic relaxation of CI formation: **(A)** steady-state (ss) SPC concentration; **(B)** time-dependent POZ concentration; **(C)** time-dependent CI formation rate constant (k_{CI}), which ultimately reaches a stable value equal to the ozonolysis rate constant (k_{oz}).

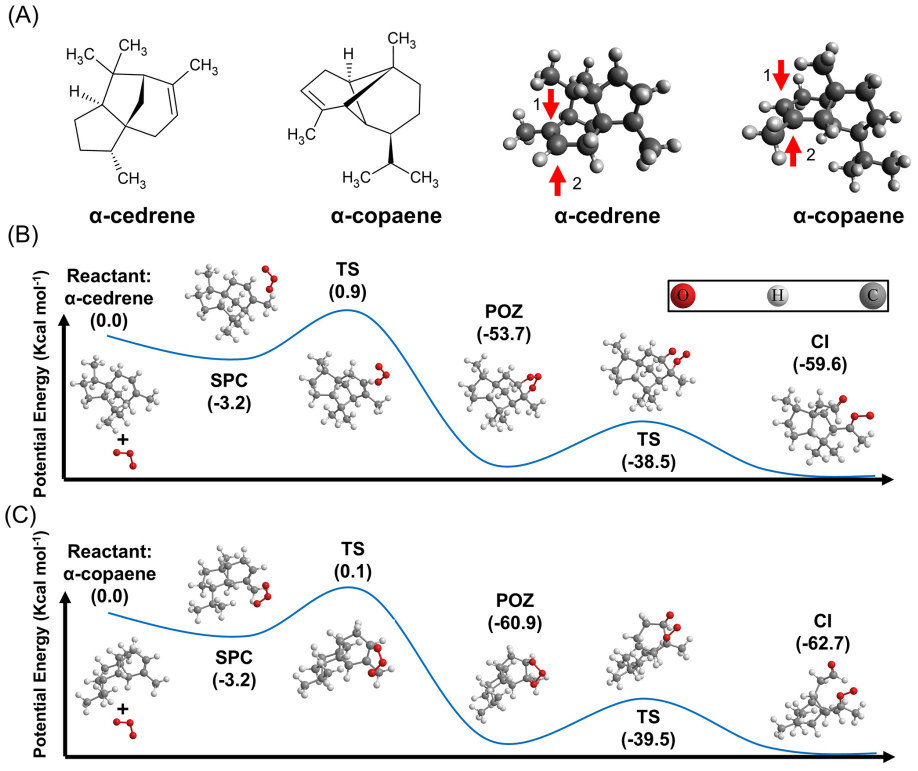


Figure 2. Examples of sesquiterpene ozonolysis kinetics: **(A)** molecular structures of α-cedrene and α-copaene with the labels of ozonolysis site 1 and 2; the "double-well" potential energy surface of the formation of **(B)** an α-cedrene-derived CI and **(C)** an α-copaene-derived CI.

only one pathway almost exclusively dominates regardless of temperature variation (Fig. 4). The branching ratios of CIs are thus governed by the branching ratios of POZ formation (Table S3), which are controlled by their corresponding SPCs (Ou and Chen, 2025). For α-cedrene, POZ2-1 exclusively produces CI isomer 1, whereas POZ2-2 exclusively produces CI isomer 2 (Fig. 5A). Since the branching ratio of POZ2-1 to POZ2-2 is approximately 9 : 1 at tropospheric temperatures (Table S3), the branching ratio of CI isomer 1 to isomer 2 from the ozonolysis of α-cedrene is also likely $\sim$ 9 : 1. Similarly, the branching ratio of CI isomer 1 to isomer 2 is likely $\sim$ 6 : 4 for α-copaene (Fig. 5B and Table S3) and $\sim$ 5 : 5 for β-caryophyllene (Fig. 5C and Table S3).

Our simulations also provide the sesquiterpene-dependent thermalized fractions of POZs (Table 1). The thermalized fractions of α-cedrene-derived POZs remain below 2 % at 1 atm and tropospheric temperatures, and therefore neglecting their kinetic relaxation does not affect the results of current atmospheric chemistry models. For β-caryophyllene, however, the thermalized fractions of the POZs exceed 90 %, so the model used to estimate CI formation rates may require adjustments that account for kinetic relaxation. For α-copaene, kinetic relaxation is likewise non-negligible for

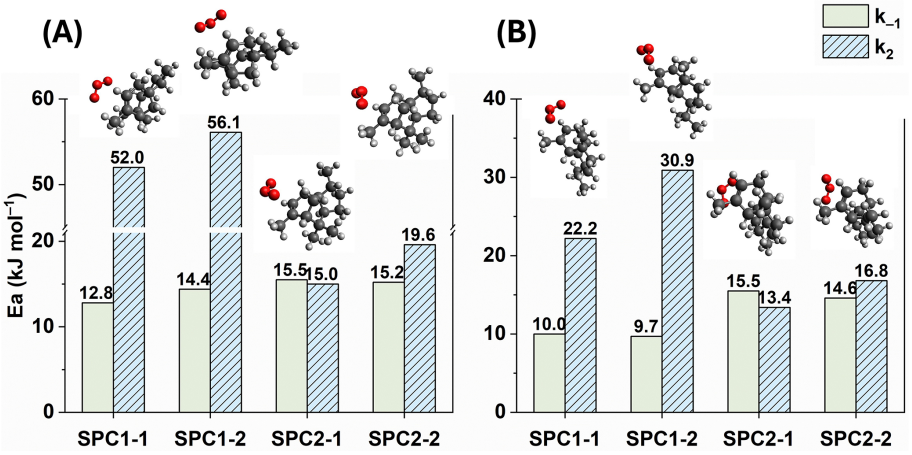


Figure 3. Fitted activation energy of k_{-1} and k_2 for all the SPCs from ozonolysis of **(A)** α-cedrene and **(B)** α-copaene.

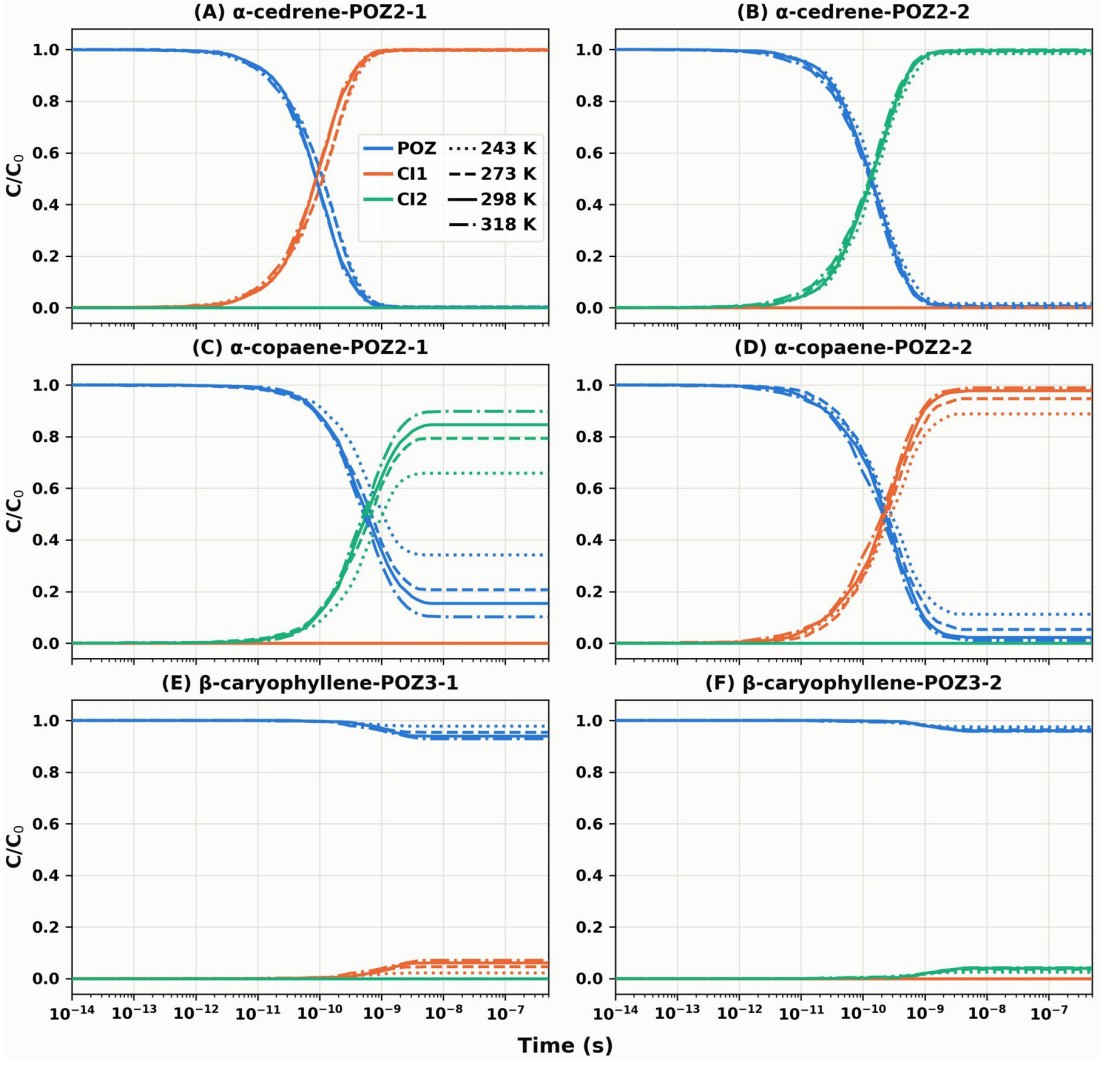


Figure 4. Simulated time-series profiles of relative concentration (C/C_0) for POZs and the resultant CIs derived from α-cedrene **(A, B)**, α-copaene **(C, D)**, and β-caryophyllene **(E, F)** at different temperatures (243, 273, 298, and 318 K).

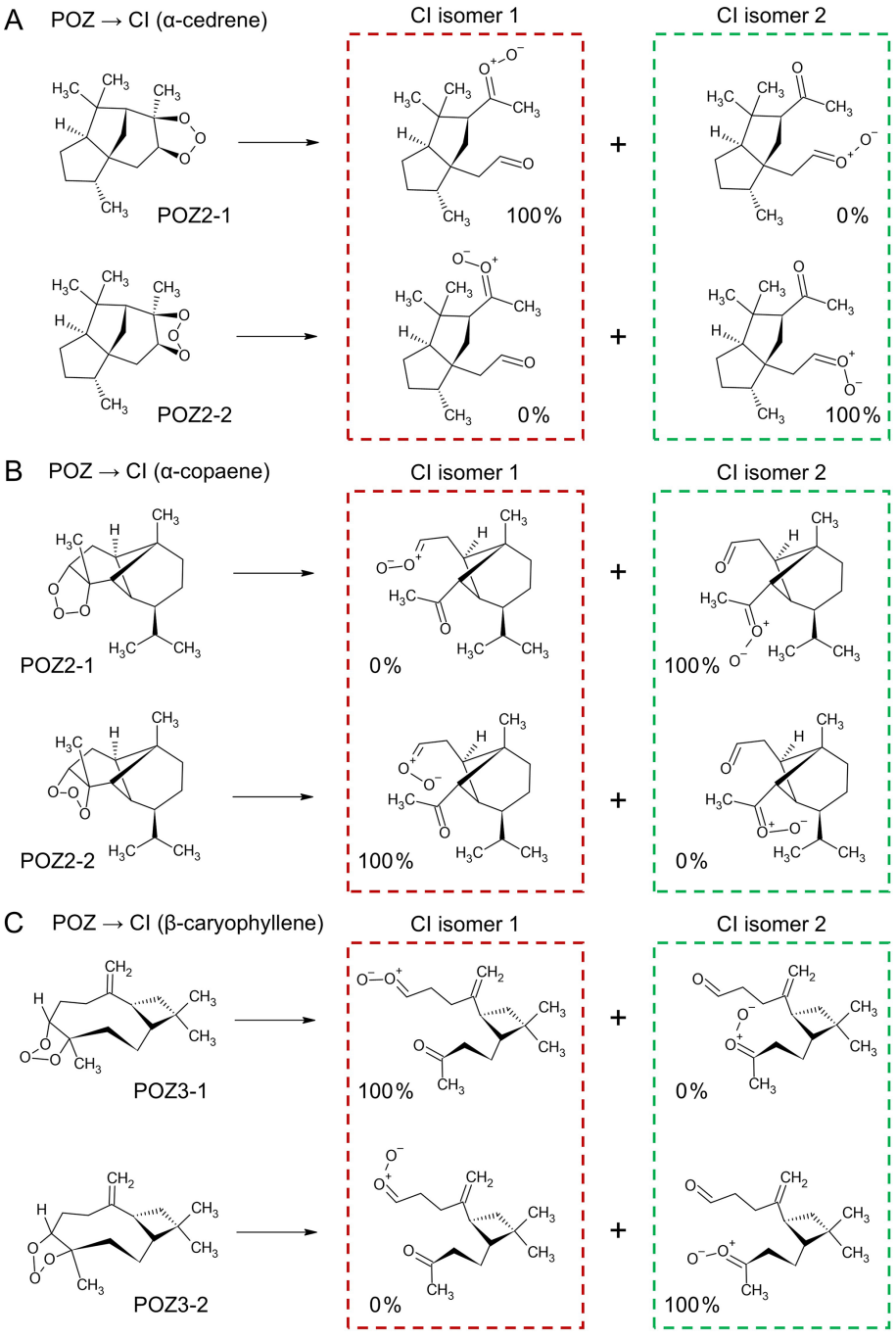


Figure 5. Structures of the predominant POZs derived from α-cedrene, α-copaene, and β-caryophyllene, and of the CIs produced by POZ decomposition with their branching ratios.

POZ2-1 but may be neglected for POZ2-2, since their thermalized fractions reach up to $\sim 34\,\%$ and remain below $12\,\%$, respectively. The differences among the sesquiterpenes are probably due to their backbones, which induce different ring strains and steric effects that influence the energy barriers related to CI formation. It is also worth noting that different CIs produced from the same sesquiterpene (e.g., α-copaene) may require different treatments for kinetic relaxation, with some potentially negligible and others requiring adjustment in next-generation atmospheric chemistry models.

Table 1. Thermalized fractions of POZs derived from α-cedrene, α-copaene, and β-caryophyllene under atmospheric conditions.

Temperature (K)	α-cedrene		α-copaene		β-caryophyllene	
	POZ2-1	POZ2-2	POZ2-1	POZ2-2	POZ3-1	POZ3-2
243	0.3 %	1.6 %	34.2 %	11.2 %	97.8 %	97.5 %
273	0.1 %	0.8 %	20.7 %	5.3 %	95.4 %	96.4 %
298	0.1 %	0.4 %	15.4 %	2.2 %	94.0 %	96.0 %
318	0.0 %	0.1 %	10.2 %	1.1 %	92.9 %	95.8 %

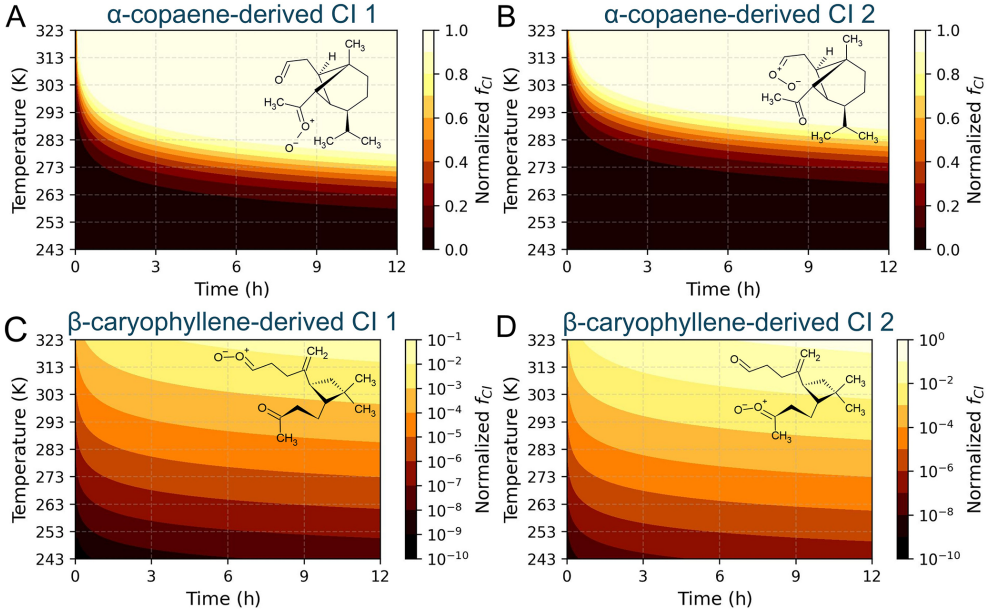


Figure 6. Kinetic relaxation of the temperature-dependent formation rate constant of **(A)** α-copaene-derived CI1, **(B)** α-copaene-derived CI2, **(C)** β-caryophyllene-derived CI1, and **(D)** β-caryophyllene-derived CI2.

3.4 Temperature Dependence of Kinetic Relaxation

Kinetic relaxation at varying temperatures is visualized by the contour of "normalized f_{CI}" (i.e., $f_{CI,i}/r_i$ as referred to Eq. 2) (Figs. 6 and S8). We found that kinetic relaxation may be more general during cold surges, while heatwaves may almost diminish the kinetic relaxation. When the temperature falls below 273 K, the normalized f_{CI} of α-copaene-derived CIs is below 0.1 for more than 1 h, but during extreme heatwaves at 318 K, the relaxation timescales are hugely reduced to several minutes (Fig. 6A and B). The strong temperature dependence is because the value of k_3 increases by 3–6 orders of magnitude as the temperature increases from 243 to 323 K (Fig. S5). A similar trend is also observed in β-caryophyllene-derived CI formation (Fig. 6C and D), wherein the normalized f_{CI} remains 1–10 orders of magnitude lower than unity across the entire temperature range. It is noted that our discussions are based on simplified cases where the pre-existing POZs are absent; the value of normalized f_{CI} can be amplified if thermalized POZs pre-exist, but the relaxation timescales remain almost unchanged (Fig. S9).

The POZ decomposition energy barriers of β-caryophyllene are the highest (Fig. S10). This distinct behavior may be related to the high ring strain of the large ring in the β-caryophyllene backbone, since the derived POZs are formed at the endocyclic double bond (Nguyen et al., 2009; Ou and Chen, 2025). The normalized f_{CI} is around 10^{-5}–10^{-3} at room temperature within 12 h, indicating that the CI formation rate constants are 3–5 orders of magnitude lower than those calculated without kinetic relaxation. The relaxation timescale, if estimated by $1/k_3$, is at least 2.6 d even under the extreme heatwaves at 323 K (Table S4). We also conducted additional simulations for β-caryophyllene-derived POZ decomposition with an initial monoenergetic distribution, representing an extreme condition in which all POZs fully obtained the excess energy from β-caryophyllene ozonolysis. In this scenario, all the POZs are decomposed, giving a k_3 value of $\sim 10^{-3}$–10^{-2} s^{-1} (Sect. S5) and a relaxation timescale of $\sim$ 2–17 min, which is longer than the ozonolysis lifetime of β-caryophyllene ($\sim$ 1–2 min) under an O_3 concentration of $\sim$ 30–60 ppb (Shu and Atkinson, 1994; Ou and Chen, 2025). Collectively, our

findings demonstrate that kinetic relaxation is non-negligible for CI formation at least from β-caryophyllene ozonolysis.

4 Conclusions

Kinetic relaxation is a previously unrecognized behavior in the formation of CIs from sesquiterpene ozonolysis. This relaxation arises from the thermalized sesquiterpene-derived POZs and potentially from non-thermalized POZs derived from certain sesquiterpenes such as β-caryophyllene. The relaxation timescale is sensitive to temperature variations and may be amplified during cold surges and suppressed during heatwaves. Under future warming scenarios (Perkins-Kirkpatrick and Lewis, 2020; Martinez-Villalobos et al., 2025) as well as less frequent cold surges (Nie et al., 2025; Blackport and Fyfe, 2024), kinetic relaxation could become less important on average, although substantial regional and seasonal variability is expected. It is also worth noting that the global trend does not necessarily represent spatiotemporal variations of temperatures; the low temperatures at high latitudes and intense cooling at night may still be possible to induce considerable kinetic relaxation. Under such conditions, ignoring kinetic relaxation may lead to overestimation of CI concentrations and therefore potentially overestimate the oxidation rates of trace gases such as SO_2 and NO_2 (Welz et al., 2012; Mauldin Iii et al., 2012; Chhantyal-Pun et al., 2020).

The decomposition of sesquiterpene-derived thermalized POZs, such as those from α-copaene and β-caryophyllene, proceeds so slowly that reactions between thermalized POZs and other gas-phase oxidants such as OH radicals may become non-negligible. This is especially relevant for polyunsaturated sesquiterpenes such as β-caryophyllene, in which the remaining carbon–carbon double bond of a POZ formed by initial ozonolysis may subsequently be attacked by OH radicals. Under typical atmospheric conditions, the estimated rate constant for OH-initiated oxidation of thermalized POZs is likely $\sim 10^{-13}$–10^{-10} cm^3 molec.$^{-1}$ s^{-1} (Mellouki et al., 2021). At a tropospheric OH concentration of $\sim 10^6$ molec. cm^{-3} (Hou et al., 2026), the first-order rate constant of this reaction reaches $\sim 10^{-7}$–10^{-4} s^{-1}, which is highly comparable to the decomposition rate constant of thermalized POZs. Moreover, the thermalized POZs could undergo reactive uptake to the aerosols or cloud droplets for heterogeneous reactions. These possibilities may open a new perspective for developing more advanced modeling schemes related to ozone chemistry and thus providing new insights into the impact of ozone pollution on the atmospheric environment.

This study also provides an additional perspective for estimating the impact of temperature variation on SOA formation. CI chemistry can contribute to SOA formation through the production of highly oxygenated organic molecules (HOMs) with extremely low volatility (Zhao et al., 2015; Richters et al., 2016a, b). The rate of HOMs formation from sesquiterpene ozonolysis may be considerably affected by the CI formation kinetics. Temperature variations could modulate the formation rate of HOMs by inducing different levels of kinetic relaxation in CI formation. A more comprehensive analysis of SOA formation should integrate detailed reaction mechanisms, temperature-dependent sesquiterpene emission factors, temperature-dependent gas-particle partitioning, and potentially new particle formation events. Among these complex factors, kinetic relaxation uniquely offers a new aspect on the CI supply flux. Overall, our study demonstrates that kinetic relaxation should be considered in atmospheric chemistry models when simulating CI chemistry under conditions characterized by strong temperature variability or low temperatures.

Data availability. All the data are available in the main text or the Supplement.

Supplement. The supplement related to this article is available online at https://doi.org/10.5194/acp-26-16571-2026-supplement.

Author contributions. H. O., Y. L. and K. C. contributed to conceptualization, computational methodology, investigation, formal analysis, and visualization. Y. S. and K. C. contributed to equation derivation. K. C. supervised the study. J. J., H. O. and Y. L. contributed to funding acquisition. H. Z., H. O. and Y. L. contributed to computational resources. H. O., Y. L., Y. S. and K. C. contributed to original draft writing. All authors contributed to draft review and editing.

Competing interests. The contact author has declared that none of the authors has any competing interests.

Disclaimer. Publisher's note: Copernicus Publications remains neutral with regard to jurisdictional claims made in the text, published maps, institutional affiliations, or any other geographical representation in this paper. The authors bear the ultimate responsibility for providing appropriate place names. Views expressed in the text are those of the authors and do not necessarily reflect the views of the publisher.

Acknowledgements. The authors would like to acknowledge the computational resources at Tsinghua University as well as those inherited from the late Professor Jun Zhao. The authors would also like to sincerely thank the editor and the reviewers for their valuable comments and constructive suggestions during the review process.

Financial support. This research has been supported by the National Natural Science Foundation of China (grant no. 22536004),

the Guangdong S&T Program (grant no. 2026B1111020001), the Key Innovation Team of Guangdong Meteorological Bureau (grant no. GRMCTD202506-ZD06), the basic research funding from the Guangzhou Institute of Tropical and Marine Meteorology of CMA (grant no. RDS202502), and the funding from the Talent Recruitment Special Project of the Shandong Meteorological Bureau (grant no. 2025SDRCYJ07).

Review statement. This paper was edited by Chiara Giorio and reviewed by Theo Kurtén and three anonymous referees.

References

Arey, J., Crowley, D. E., Crowley, M., Resketo, M., and Lester, J.: Hydrocarbon emissions from natural vegetation in California's South Coast Air Basin, Atmos. Environ., 29, 2977–2988, https://doi.org/10.1016/1352-2310(95)00137-N, 1995.

Barker, J. R.: Multiple-Well, multiple-path unimolecular reaction systems. I. MultiWell computer program suite, Int. J. Chem. Kinet., 33, 232–245, https://doi.org/10.1002/kin.1017, 2001.

Barker, J. R.: Energy transfer in master equation simulations: A new approach, Int. J. Chem. Kinet., 41, 748–763, https://doi.org/10.1002/kin.20447, 2009.

Barker, J. R., Yoder, L. M., and King, K. D.: Vibrational Energy Transfer Modeling of Nonequilibrium Polyatomic Reaction Systems, J. Phys. Chem. A, 105, 796–809, https://doi.org/10.1021/jp002077f, 2001.

Blackport, R. and Fyfe, J. C.: Amplified warming of North American cold extremes linked to human-induced changes in temperature variability, Nat. Commun., 15, 5864, https://doi.org/10.1038/s41467-024-49734-8, 2024.

Chen, X., Gong, D., Liu, S., Meng, X., Li, Z., Lin, Y., Li, Q., Xu, R., Chen, S., Chang, Q., Ma, F., Ding, X., Deng, S., Zhang, C., Wang, H., and Wang, B.: In-situ online investigation of biogenic volatile organic compounds emissions from tropical rainforests in Hainan, China, Sci. Total Environ., 954, 176668, https://doi.org/10.1016/j.scitotenv.2024.176668, 2024.

Chhantyal-Pun, R., Khan, M. A. H., Taatjes, C. A., Percival, C. J., Orr-Ewing, A. J., and Shallcross, D. E.: Criegee intermediates: production, detection and reactivity, Int. Rev. Phys. Chem., 39, 385–424, https://doi.org/10.1080/0144235X.2020.1792104, 2020.

Chuong, B., Zhang, J., and Donahue, N. M.: Cycloalkene Ozonolysis: Collisionally Mediated Mechanistic Branching, J. Am. Chem. Soc., 126, 12363–12373, https://doi.org/10.1021/ja0485412, 2004.

Cox, R. A., Ammann, M., Crowley, J. N., Herrmann, H., Jenkin, M. E., McNeill, V. F., Mellouki, A., Troe, J., and Wallington, T. J.: Evaluated kinetic and photochemical data for atmospheric chemistry: Volume VII – Criegee intermediates, Atmos. Chem. Phys., 20, 13497–13519, https://doi.org/10.5194/acp-20-13497-2020, 2020.

Cremer, D.: Theoretical determination of molecular structure and conformation. 8. Energetics of the ozonolysis reaction. Primary ozonide vs. carbonyl oxide control of stereochemistry, J. Am. Chem. Soc., 103, 3627–3633, https://doi.org/10.1021/ja00403a002, 1981.

Criegee, R.: Mechanism of Ozonolysis, Angew. Chem. Int. Ed., 14, 745–752, https://doi.org/10.1002/anie.197507451, 1975.

Davis, M. E., Drake, W., Vimal, D., and Stevens, P. S.: Experimental and theoretical studies of the kinetics of the reactions of OH and OD with acetone and acetone-d6 at low pressure, J. Photoch. Photobio. A, 176, 162–171, https://doi.org/10.1016/j.jphotochem.2005.08.030, 2005.

Dekermenjian, M., Allen, D. T., Atkinson, R., and Arey, J.: FTIR Analysis of Aerosol Formed in the Ozone Oxidation of Sesquiterpenes, Aerosol Sci. Tech., 30, 349–363, https://doi.org/10.1080/027868299304552, 1999.

Docherty, K. S., Wu, W., Lim, Y. B., and Ziemann, P. J.: Contributions of Organic Peroxides to Secondary Aerosol Formed from Reactions of Monoterpenes with O_3, Environ. Sci. Technol., 39, 4049–4059, https://doi.org/10.1021/es050228s, 2005.

Donahue, N. M., Drozd, G. T., Epstein, S. A., Presto, A. A., and Kroll, J. H.: Adventures in ozoneland: down the rabbit-hole, Phys. Chem. Chem. Phys., 13, 10848–10857, https://doi.org/10.1039/C0CP02564J, 2011.

Duhl, T. R., Helmig, D., and Guenther, A.: Sesquiterpene emissions from vegetation: a review, Biogeosciences, 5, 761–777, https://doi.org/10.5194/bg-5-761-2008, 2008.

Dunning Jr., T. H.: Gaussian basis sets for use in correlated molecular calculations. I. The atoms boron through neon and hydrogen, J. Chem. Phys., 90, 1007–1023, https://doi.org/10.1063/1.456153, 1989.

Frazier, G., McGlynn, D. F., Barry, L. E., Lerdau, M., Pusede, S. E., and Isaacman-VanWertz, G.: Composition, concentration, and oxidant reactivity of sesquiterpenes in the southeastern U.S., Environ. Sci. Atmos., 2, 1208–1220, https://doi.org/10.1039/D2EA00059H, 2022.

Gao, L., Song, J., Mohr, C., Huang, W., Vallon, M., Jiang, F., Leisner, T., and Saathoff, H.: Kinetics, SOA yields, and chemical composition of secondary organic aerosol from β-caryophyllene ozonolysis with and without nitrogen oxides between 213 and 313 K, Atmos. Chem. Phys., 22, 6001–6020, https://doi.org/10.5194/acp-22-6001-2022, 2022.

Gong, Y. and Chen, Z.: Quantification of the role of stabilized Criegee intermediates in the formation of aerosols in limonene ozonolysis, Atmos. Chem. Phys., 21, 813–829, https://doi.org/10.5194/acp-21-813-2021, 2021.

Hakala, J. and Donahue, N. M.: Carbonyl Oxide Stabilization from Trans Alkene and Terpene Ozonolysis, J. Phys. Chem. A, 127, 8530–8543, https://doi.org/10.1021/acs.jpca.3c03650, 2023.

Hippler, H., Troe, J., and Wendelken, H. J.: Collisional deactivation of vibrationally highly excited polyatomic molecules. II. Direct observations for excited toluene, J. Chem. Phys., 78, 6709–6717, https://doi.org/10.1063/1.444670, 1983.

Hou, X., Hossaini, R., Wild, O., Mazzeo, A., Pope, R. J., Wang, Y., Wang, S., Zhao, Y., Lee, J., Zhu, B., Zhao, T., and Pandey, A. K.: Tropospheric OH and its trends: new insight into atmospheric processes and implications for methane lifetime, Atmos. Chem. Phys., 26, 13767–13793, https://doi.org/10.5194/acp-26-13767-2026, 2026.

Iyer, S., Rissanen, M. P., Valiev, R., Barua, S., Krechmer, J. E., Thornton, J., Ehn, M., and Kurtén, T.: Molecular mechanism for rapid autoxidation in α-pinene ozonolysis, Nat. Commun., 12, 878, https://doi.org/10.1038/s41467-021-21172-w, 2021.

Jaoui, M., Leungsakul, S., and Kamens, R. M.: Gas and Particle Products Distribution from the Reaction of β-Caryophyllene with Ozone, J. Atmos. Chem., 45, 261–287, https://doi.org/10.1023/A:1024263430285, 2003.

Jaoui, M., Sexton, K. G., and Kamens, R. M.: Reaction of α-cedrene with ozone: mechanism, gas and particulate products distribution, Atmos. Environ., 38, 2709–2725, https://doi.org/10.1016/j.atmosenv.2004.02.007, 2004.

Jaoui, M., Kleindienst, T. E., Docherty, K. S., Lewandowski, M., and Offenberg, J. H.: Secondary organic aerosol formation from the oxidation of a series of sesquiterpenes: a-cedrene, β-caryophyllene, a-humulene and a-farnesene with O_3, OH and NO_3 radicals, Environ. Chem., 10, 178–193, https://doi.org/10.1071/EN13025, 2013.

Jaoui, M., Lewandowski, M., Offenberg, J. H., Docherty, K. S., and Kleindienst, T. E.: Ozonolysis of α/β-farnesene mixture: Analysis of gas-phase and particulate reaction products, Atmos. Environ., 169, 175–192, https://doi.org/10.1016/j.atmosenv.2017.08.065, 2017.

Johnson, D. and Marston, G.: The gas-phase ozonolysis of unsaturated volatile organic compounds in the troposphere, Chem. Soc. Rev., 37, 699–716, https://doi.org/10.1039/B704260B, 2008.

Kanawati, B., Herrmann, F., Joniec, S., Winterhalter, R., and Moortgat, G. K.: Mass spectrometric characterization of β-caryophyllene ozonolysis products in the aerosol studied using an electrospray triple quadrupole and time-of-flight analyzer hybrid system and density functional theory, Rapid Commun. Mass Sp., 22, 165–186, https://doi.org/10.1002/rcm.3340, 2008.

Khan, M. A. H., Percival, C. J., Caravan, R. L., Taatjes, C. A., and Shallcross, D. E.: Criegee intermediates and their impacts on the troposphere, Environ. Sci.-Proc. Imp., 20, 437–453, https://doi.org/10.1039/C7EM00585G, 2018.

Kim, D., Stevens, P. S., and Hites, R. A.: Rate Constants for the Gas-Phase Reactions of OH and O_3 with β-Ocimene, β-Myrcene, and α- and β-Farnesene as a Function of Temperature, J. Phys. Chem. A, 115, 500–506, https://doi.org/10.1021/jp111173s, 2011.

Lwande, W., McDowell, P. G., Amiani, H., and Amoke, P.: Analysis of airborne volatiles of cowpea, Phytochemistry, 28, 421–423, https://doi.org/10.1016/0031-9422(89)80025-1, 1989.

Martinez-Villalobos, C., Fu, D., Loikith, P. C., and Neelin, J. D.: Accelerating increase in the duration of heatwaves under global warming, Nat. Geosci., 18, 716–723, https://doi.org/10.1038/s41561-025-01737-w, 2025.

Mauldin Iii, R. L., Berndt, T., Sipilä, M., Paasonen, P., Petäjä, T., Kim, S., Kurtén, T., Stratmann, F., Kerminen, V. M., and Kulmala, M.: A new atmospherically relevant oxidant of sulphur dioxide, Nature, 488, 193–196, https://doi.org/10.1038/nature11278, 2012.

Mellouki, A., Ammann, M., Cox, R. A., Crowley, J. N., Herrmann, H., Jenkin, M. E., McNeill, V. F., Troe, J., and Wallington, T. J.: Evaluated kinetic and photochemical data for atmospheric chemistry: volume VIII – gas-phase reactions of organic species with four, or more, carbon atoms ($\geq C_4$), Atmos. Chem. Phys., 21, 4797–4808, https://doi.org/10.5194/acp-21-4797-2021, 2021.

Nangia, P. S. and Benson, S. W.: Thermochemistry and kinetics of ozonation reactions, J. Am. Chem. Soc., 102, 3105–3115, https://doi.org/10.1021/ja00529a037, 1980.

Neese, F.: The ORCA program system, WIRes Comput. Mol. Sci., 2, 73–78, https://doi.org/10.1002/wcms.81, 2012.

Neese, F., Wennmohs, F., Hansen, A., and Becker, U.: Efficient, approximate and parallel Hartree–Fock and hybrid DFT calculations. A "chain-of-spheres" algorithm for the Hartree–Fock exchange, Chem. Phys., 356, 98–109, https://doi.org/10.1016/j.chemphys.2008.10.036, 2009.

Nguyen, T. L., Winterhalter, R., Moortgat, G., Kanawati, B., Peeters, J., and Vereecken, L.: The gas-phase ozonolysis of β-caryophyllene ($C_{15}H_{24}$). Part II: A theoretical study, Phys. Chem. Chem. Phys., 11, 4173–4183, https://doi.org/10.1039/B817913A, 2009.

Nie, Y., Sun, Y., Zhang, X., and Chen, G.: Human-induced changes in extreme cold surges across the Northern Hemisphere, Nat. Commun., 16, 8086, https://doi.org/10.1038/s41467-025-62576-2, 2025.

Ou, H. and Chen, K.: Atmospheric Temperature Dependence of β-Caryophyllene Ozonolysis Kinetics Is Governed by Stabilized Prereactive Complexes, J. Phys. Chem. A, 129, 9982–9990, https://doi.org/10.1021/acs.jpca.5c05523, 2025.

Ou, H., Sha, Y., Deng, T., Zhou, H., and Chen, K.: Extreme Temperature Divergently Alters Ozonolysis Kinetics of Atmospheric Cadinenes, ACS ES&T Air, 3, 1586–1595, https://doi.org/10.1021/acsestair.6c00017, 2026.

Perkins-Kirkpatrick, S. E. and Lewis, S. C.: Increasing trends in regional heatwaves, Nat. Commun., 11, 3357, https://doi.org/10.1038/s41467-020-16970-7, 2020.

Reinnig, M.-C., Warnke, J., and Hoffmann, T.: Identification of organic hydroperoxides and hydroperoxy acids in secondary organic aerosol formed during the ozonolysis of different monoterpenes and sesquiterpenes by on-line analysis using atmospheric pressure chemical ionization ion trap mass spectrometry, Rapid Commun. Mass Sp., 23, 1735–1741, https://doi.org/10.1002/rcm.4065, 2009.

Richters, S., Herrmann, H., and Berndt, T.: Gas-phase rate coefficients of the reaction of ozone with four sesquiterpenes at 295 ± 2 K, Phys. Chem. Chem. Phys., 17, 11658–11669, https://doi.org/10.1039/C4CP05542J, 2015.

Richters, S., Herrmann, H., and Berndt, T.: Different pathways of the formation of highly oxidized multifunctional organic compounds (HOMs) from the gas-phase ozonolysis of β-caryophyllene, Atmos. Chem. Phys., 16, 9831–9845, https://doi.org/10.5194/acp-16-9831-2016, 2016a.

Richters, S., Herrmann, H., and Berndt, T.: Highly Oxidized RO_2 Radicals and Consecutive Products from the Ozonolysis of Three Sesquiterpenes, Environ. Sci. Technol., 50, 2354–2362, https://doi.org/10.1021/acs.est.5b05321, 2016b.

Riplinger, C. and Neese, F.: An efficient and near linear scaling pair natural orbital based local coupled cluster method, J. Chem. Phys., 138, 034106, https://doi.org/10.1063/1.4773581, 2013.

Shu, Y. and Atkinson, R.: Rate constants for the gas-phase reactions of O3 with a series of Terpenes and OH radical formation from the O3 reactions with Sesquiterpenes at 296 ± 2 K, Int. J. Chem. Kinet., 26, 1193–1205, https://doi.org/10.1002/kin.550261207, 1994.

Shu, Y. and Atkinson, R.: Atmospheric lifetimes and fates of a series of sesquiterpenes, J. Geophys. Res.-Atmos., 100, 7275–7281, https://doi.org/10.1029/95JD00368, 1995.

Taatjes, C. A., Shallcross, D. E., and Percival, C. J.: Research frontiers in the chemistry of Criegee intermediates and tropo-

spheric ozonolysis, Phys. Chem. Chem. Phys., 16, 1704–1718, https://doi.org/10.1039/C3CP52842A, 2014.

Talukdar, R. K., Gierczak, T., McCabe, D. C., and Ravishankara, A. R.: Reaction of Hydroxyl Radical with Acetone. 2. Products and Reaction Mechanism, J. Phys. Chem. A, 107, 5021–5032, https://doi.org/10.1021/jp0273023, 2003.

Tardy, D. C. and Rabinovitch, B. S.: Intermolecular vibrational energy transfer in thermal unimolecular systems, Chem. Rev., 77, 369–408, https://doi.org/10.1021/cr60307a004, 1977.

Vereecken, L. and Francisco, J. S.: Theoretical studies of atmospheric reaction mechanisms in the troposphere, Chem. Soc. Rev., 41, 6259–6293, https://doi.org/10.1039/C2CS35070J, 2012.

Weaver, A. B. and Alexeenko, A. A.: Revised Variable Soft Sphere and Lennard-Jones Model Parameters for Eight Common Gases up to 2200 K, J. Phys. Chem. Ref. Data, 44, 023103, https://doi.org/10.1063/1.4921245, 2015.

Weigend, F. and Ahlrichs, R.: Balanced basis sets of split valence, triple zeta valence and quadruple zeta valence quality for H to Rn: Design and assessment of accuracy, Phys. Chem. Chem. Phys., 7, 3297–3305, https://doi.org/10.1039/B508541A, 2005.

Weigend, F., Köhn, A., and Hättig, C.: Efficient use of the correlation consistent basis sets in resolution of the identity MP2 calculations, J. Chem. Phys., 116, 3175–3183, https://doi.org/10.1063/1.1445115, 2002.

Welz, O., Savee, J. D., Osborn, D. L., Vasu, S. S., Percival, C. J., Shallcross, D. E., and Taatjes, C. A.: Direct Kinetic Measurements of Criegee Intermediate (CH2OO) Formed by Reaction of CH_2I with O_2, Science, 335, 204–207, https://doi.org/10.1126/science.1213229, 2012.

Winterhalter, R., Herrmann, F., Kanawati, B., Nguyen, T. L., Peeters, J., Vereecken, L., and Moortgat, G. K.: The gas-phase ozonolysis of β-caryophyllene ($C_{15}H_{24}$). Part I: an experimental study, Phys. Chem. Chem. Phys., 11, 4152–4172, https://doi.org/10.1039/B817824K, 2009.

Wong, B. M., Matheu, D. M., and Green, W. H.: Temperature and Molecular Size Dependence of the High-Pressure Limit, J. Phys. Chem. A, 107, 6206–6211, https://doi.org/10.1021/jp034165g, 2003.

Yao, L., Ma, Y., Wang, L., Zheng, J., Khalizov, A., Chen, M., Zhou, Y., Qi, L., and Cui, F.: Role of stabilized Criegee Intermediate in secondary organic aerosol formation from the ozonolysis of α-cedrene, Atmos. Environ., 94, 448–457, https://doi.org/10.1016/j.atmosenv.2014.05.063, 2014.

Yao, Q., Sun, X.-H., Li, Z.-R., Chen, F.-F., and Li, X.-Y.: Pressure-Dependent Rate Rules for Intramolecular H-Migration Reactions of Hydroperoxyalkylperoxy Radicals in Low Temperature, J. Phys. Chem. A, 121, 3001–3018, https://doi.org/10.1021/acs.jpca.6b10818, 2017.

Yee, L. D., Isaacman-VanWertz, G., Wernis, R. A., Meng, M., Rivera, V., Kreisberg, N. M., Hering, S. V., Bering, M. S., Glasius, M., Upshur, M. A., Gray Bé, A., Thomson, R. J., Geiger, F. M., Offenberg, J. H., Lewandowski, M., Kourtchev, I., Kalberer, M., de Sá, S., Martin, S. T., Alexander, M. L., Palm, B. B., Hu, W., Campuzano-Jost, P., Day, D. A., Jimenez, J. L., Liu, Y., McKinney, K. A., Artaxo, P., Viegas, J., Manzi, A., Oliveira, M. B., de Souza, R., Machado, L. A. T., Longo, K., and Goldstein, A. H.: Observations of sesquiterpenes and their oxidation products in central Amazonia during the wet and dry seasons, Atmos. Chem. Phys., 18, 10433–10457, https://doi.org/10.5194/acp-18-10433-2018, 2018.

Zhao, Y. and Truhlar, D. G.: The M06 suite of density functionals for main group thermochemistry, thermochemical kinetics, noncovalent interactions, excited states, and transition elements: two new functionals and systematic testing of four M06-class functionals and 12 other functionals, Theor. Chem. Acc., 120, 215–241, https://doi.org/10.1007/s00214-007-0310-x, 2008.

Zhao, Y., Wingen, L. M., Perraud, V., Greaves, J., and Finlayson-Pitts, B. J.: Role of the reaction of stabilized Criegee intermediates with peroxy radicals in particle formation and growth in air, Phys. Chem. Chem. Phys., 17, 12500–12514, https://doi.org/10.1039/C5CP01171J, 2015.

Zhao, Y., Wingen, L. M., Perraud, V., and Finlayson-Pitts, B. J.: Phase, composition, and growth mechanism for secondary organic aerosol from the ozonolysis of α-cedrene, Atmos. Chem. Phys., 16, 3245–3264, https://doi.org/10.5194/acp-16-3245-2016, 2016.